ISSN 2176-5480

22nd International Congress of Mechanical Engineering (COBEM 2013)
November 3-7, 2013, Ribeirão Preto, SP, Brazil

DESIGN OF THREE DIMENSIONAL AUTOMATIC FLIGHT SYSTEM FOR CLIMB, CRUISE AND DESCENT

Lucas Emídio Roque da Silva
Instituto Tecnológico de Aeronáutica - Aeronautical Engineering Division, CEP 12.228-900, São José dos Campos, SP, Brazil
lucaserds@gmail.com
Pedro Paglione
Instituto Tecnológico de Aeronáutica - Aeronautical Engineering Division, CEP 12.228-900, São José dos Campos, SP, Brazil
paglione@ita.br

Abstract. *Analysis of the recent history of commercial passenger transport aircraft makes it possible to notice that fly-by-wire technology has become the new standard for manufactures. Fly-by-wire systems allow the implementation of complex automatic flight control systems, whose objective is to provide optimal handling qualities for specific flight phases, while reducing operational costs and increasing safety and passenger comfort. The present work aims to design a control system capable of rejecting disturbances and optimal tracking of typical trajectories operated by commercial aircraft.*
The proposed model to simulate the aircraft dynamics is described by nonlinear ordinary differential equations in a body-fixed reference system. The problem is complex and hard to solve therefore it is necessary to linearize the model in multiple operational points throughout the flight envelope. Based on each linear model, the control gains are designed using optimization techniques and then scheduled in order to cover the operational envelope and the aircraft mass variation. The climb, descent and cruise trajectories, as well as the capture trajectory between these phases, are specified according to typical profiles and implemented for longitudinal and lateral-directional modes.
The resulting system is simulated using the nonlinear model to verify its response to wind disturbances. As a conclusion, a robustness analysis is performed, presented and discussed, emphasizing the validity of the methodology in the design of flight control systems.

Keywords: *Automatic flight control, climb, cruise, descent, aircraft dynamics*

1. INTRODUCTION

The constant growth in operation performance requirements made commercial aircraft increasingly less stable. The controllability criteria became gradually more complex, motivating, in 1912, the first autopilot project and, in 1913, the classic control theory (Stevens & Lewis, 1992).

The application of control theory on aircraft industry derived the necessity of a more sophisticated dynamic analysis of the systems, what allowed the solving of a number of problems, expanding the flight envelope, the stability, the controllability and the flight qualities criteria. Stability Augmentation Systems (SAS) became necessary to cope with greater sizes and constant desires to decrease static stability margin in order to increase performance. From the aerodynamic point of view, SAS modify one or more stability derivatives throughout the positioning of the flight control surfaces as a response to an aircraft movement or to an external disturbance (Etkin, 1959). The Controllability Augmentation Systems (CAS) later appeared applying the same principle but aiming to decrease crew work load.

The fast evolution of computers allowed the development of Fly-By-Wire (FBW) systems. According to Sutherland (1968), FBW systems may be described as the ones where there is a complete replacement of the mechanical linkage between the pilots input system and the control surface actuators. Instead, the pilots commands are converted by digital computers into control objectives and compared to the aircraft current state - inferred from inertial and anemometrical sensors (Fielding, 2000). The control laws are then able to specify the control surfaces position and the suitable thrust that guarantee the best flying qualities and performance.

The main advantage of FBW systems is exactly the possibility to use the control laws to obtain the aircraft desired closed loop dynamic all over the flight envelope (Briere, Favre, & Traverse, 2001) - that constitutes the current work main objective. The variation of mass and altitude inside the flight envelope are taken into consideration on the control laws design. The calculated gains for a wide range of these parameters are scheduled along a flight trajectory made of climb, cruise and descent, including the capture phases between these conditions. The resulting design is evaluated using certified methods and is later tested on a non-linear model under the influence of wind disturbances, where it is possible to evaluate the benefits of this approach.

2. AUTOMATIC CONTROL SYSTEMS

The modern aircraft operation throughout the flight envelope may cause great variation in parameters such as dynamic and static pressure, aerodynamic coefficients and mass. As a consequence of the change in these parameters,

ISSN 2176-5480

the aircraft dynamic may suffer relevant alterations, making stable and damped modes become unstable or highly oscillatory. It may generate a higher crew workload, passenger discomfort, reduction of aerodynamic performance and growth of fuel consumption.

The aircraft dynamic modes may be separated in two different groups. The first one includes rotational modes – short period, roll subsidence and Dutch roll. The second one includes phugoid and spiral, very much slower than the modes in the first group. If the rotational modes, due to their high frequency, become low damped or unstable, Stability Augmentation Systems (SAS) may be necessary to adjust frequency and damping, allowing an adequate flight quality. The slower modes, on the other hand, although controllable by the crew, may be set under control of the autopilot, decreasing crew workload.

Automatic control systems are designed to move the poles that characterize each aerodynamic mode. When the automatic control loop is closed, it is possible to change the open loop poles, defined by the aircraft geometry, mass, control surfaces performance, pilot work, flight condition, mission, etc.

The next section details the theory behind the automatic control systems designed in the present work.

2.1 Control Laws Design

If properly designed, a control law based on negative feedback with constant gains is able to stabilize unstable systems, damp oscillatory poles, increase response velocity, reject disturbances, track trajectories, etc.

In the present work, four different automatic control systems are designed:

- An autopilot for cruise that keeps constant altitude and constant aerodynamic velocity while rejecting wind disturbances;
- An autopilot for climb/descent that aims to track a trajectory keeping constant the calibrated airspeed;
- An autopilot for capture, based on a reference model for altitude and velocity, responsible by the transition between climb and cruise and between cruise and descent;
- An autopilot for bank angle hold;

Each autopilot system includes a longitudinal Stability Augmentation System controlling pitch rate and pitch angle and a lateral-directional Stability Augmentation System controlling roll rate and yaw rate. The next three subsections describe the control law theories behind the designed automatic control systems. They relate the open loop plant natural dynamic to the desired dynamic for the closed loop system.

Firstly, suppose the open loop system is trimmed on an equilibrium condition and can be represented by the state space Eq. (1).

$$\begin{aligned} \dot{x} &= Ax + Bu \\ y &= Cx \\ z &= Hx \end{aligned} \tag{1}$$

Where y are the measured outputs and z are the performance outputs. Figure 1 shows a basic control system.

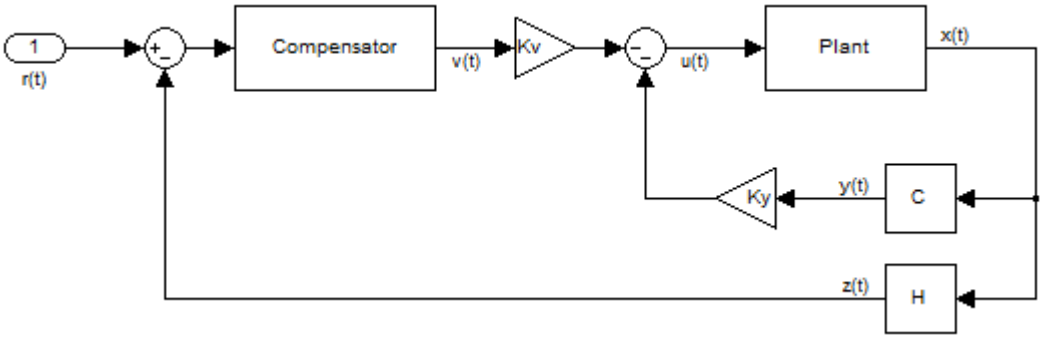

Figure 1. Basic Automatic Control System

The designed compensator can be represented by Eq. (2).

$$\begin{aligned} \dot{w} &= Fw + Ge \\ v &= Dw + Je \end{aligned} \tag{2}$$

ISSN 2176-5480

Where $e(t)=r(t)-z(t)=r(t)-Hx(t)$ and F, G, D and J are matrixes that may be chosen according to the desired structure for the compensator. The augmented system, equivalent to plant and compensator, will then be written as shown in Eq. (3).

$$\begin{aligned}
&\begin{bmatrix}\dot{x}\\ \dot{w}\end{bmatrix}=\begin{bmatrix}A & 0\\ -GH & F\end{bmatrix}\begin{bmatrix}x\\ w\end{bmatrix}+\begin{bmatrix}B\\ 0\end{bmatrix}u+\begin{bmatrix}0\\ G\end{bmatrix}r \Rightarrow \dot{x}_a = A_a x_a + B_a u + G_a r\\
&\begin{bmatrix}y\\ v\end{bmatrix}=\begin{bmatrix}C & 0\\ -JH & D\end{bmatrix}\begin{bmatrix}x\\ w\end{bmatrix}+\begin{bmatrix}0\\ J\end{bmatrix}r \Rightarrow y_a = C_a x_a + F_a r\\
&z=\begin{bmatrix}H & 0\end{bmatrix}\begin{bmatrix}x\\ w\end{bmatrix} \Rightarrow z = H_a x_a
\end{aligned} \tag{3}$$

Figure 1 allows the conclusion of Eq. (4).

$$u=-K_y y-K_v v=-\begin{bmatrix}K_y & K_v\end{bmatrix}\begin{bmatrix}y\\ v\end{bmatrix}=-Ky_a=-KC_a x_a-KF_a r \tag{4}$$

Replacing u on the previous equations, it is possible to find the close loop system described by Eq. (5).

$$\dot{x}_a=\left(A_a-B_a KC_a\right)x_a+\left(G_a-B_a KF_a\right)r=A_c x_a+B_c r \tag{5}$$

2.1.1 Linear Quadratic Regulator for Output Tracking

Frequently, when designing aircraft control systems, it is interesting to design a compensator to track a specific trajectory while rejecting eventual disturbances. This situation, on the present study, applies to the Stability Augmentation Systems and to the Autopilots. For the system in Figure 1, one may propose a linear quadratic regulator for output tracking whose structure may be chosen freely. The gains are found numerically throughout the minimization of a performance index given by Eq. (6), seen in Stevens & Lewis, (1992).

$$J=\frac{1}{2}\int_0^\infty\left(\tilde{x}^T Q\tilde{x}+\tilde{u}^T R\tilde{u}\right)dt+\frac{1}{2}\tilde{e}^T V\tilde{e} \tag{6}$$

Where $\tilde{x}$, $\tilde{u}$ and $\tilde{e}$ are the deviation of each variable related to the stationary state. Q, R and V must be arbitrarily selected, which may be considered as a disadvantage of this method. However, if the stationary sate error is not a concern, $V=0$. If one of the objectives is to minimize the error deviation, one may set $Q=H^T H$. So the only left parameter is to be selected is R, the weight of the control variables. In order to find the optimal gains, one must find, firstly, a stabilizing guess K. From this guess, one may solve the Lyapunov Eq. (7) for P (Stevens & Lewis, 1992).

$$A_c^T P+PA_c+Q+C_a^T K^T RKC_a=0 \tag{7}$$

Replacing P on the next equation, where r_0 is the module of the reference step $r(t)$, one may find Eq. (8).

$$\begin{aligned}
&X=A_c^{-1}B_c r_o r_0^T B_c^T A_c^{-T}\\
&J=\frac{1}{2}tr\left(PX\right)+\frac{1}{2}\tilde{e}^T V\tilde{e}
\end{aligned} \tag{8}$$

The three equation are solved iteratively aiming to minimize J. For minimization, it was used the *fmincon* MATLAB® command, what allowed the determination of the K gains.

2.1.2 Linear Quadratic Regulator for Output Tracking with Time-Depending Weighting

The minimization of the linear quadratic index, discussed on the previous subsection, in some cases, may generate a slow pole in the closed loop system. In order to solve this issue, one may develop an objective function that takes into

ISSN 2176-5480

consideration an additional penalty for the slow residual errors, weighting the states by the time, as in Eq. (9) (Stevens & Lewis, 1992).

$$J = \frac{1}{2}\int_0^\infty \left(t^k \tilde{x}^T P \tilde{x} + \tilde{x}^T \left(Qx + C_a^T K^T RKC\right)\tilde{x}\right)dt \tag{9}$$

In this present study, $Q = 0$ and $P = H^T H$, considering the system observability. So the design decision only includes k, the time weight, and R, the control inputs weight. The higher the k, the higher the penalty put on the errors that happen lately on the system output, suppressing the slow pole effect. As to find the gains that will minimize the objective function, one must solve iteratively Eq. (10).

$$\begin{aligned} &A_c^T P_k + P_k A_c + k! P_{k-1} + Q + C_a^T K^T RKC_a = 0 \quad (solve\ for\ P_k) \\ &X = A_c^{-1} B_c r_o r_0^T B_c^T A_c^{-T} \\ &J = \frac{1}{2} tr\left(P_k X\right) \end{aligned} \tag{10}$$

2.1.3 ITAE Minimization

The minimization of the Integral Time Absolute Error (ITAE) index follows the same principles applied to Linear Quadratic Index minimization and applies to similar cases. This method, opposed to the previous ones, does not depend on a design variable, whose arbitrary choice may impact directly on the design. The main disadvantage is it is not possible to regulate the control usage. ITAE minimization technique, nevertheless, is able to generate compensators with high disturb cancellation properties, low overshoot and high robustness. There is a number of performance indexes, such as ISE (Integral Square Error), IAE (Integral Absolute Error), etc. ITAE takes into consideration the errors that take too much time to tend to zero, what is relevant for the projects where it is applied.

So the objective is to find the K gains that minimize the ITAE index, describe by Eq. (11) (Awouda).

$$ITAE = \int_0^\infty t\left|e(t)\right|dt \tag{11}$$

Figure 1 describes the same system model, where it is possible to conclude $e(t) = r(t) - z(t) = r(t) - H_a x_a(t)$. As on the previous techniques, it was used the *fmincon* MATLAB® function, able to find the constrained minimal value of a function.

3. MODELING

A mathematical model with some degree of reliability is an import prerequisite for any control laws design, whatever the employed method or technique. Once the control law design is completed, one may evaluate the project regarding sensibility to modeling parameters, what allows increasing the knowledge about the closed loop system and, if necessary, investing in increasing the model fidelity (North Atlantic Treaty Organization, 2000).

The present work is based on a mathematical model for Airbus A320, a narrow-body commercial aircraft. In order to deduce the aircraft rigid body equations, one must consider a body reference system, an inertial reference system and an aerodynamic reference system. The Force equations may then be written as shown on Eq. (12).

$$\begin{aligned} \dot{u} &= -qw + vr - g\sin(\theta) + \left(X + F_T \cos\alpha_T\right)/M \\ \dot{v} &= -ru + wp - g\cos(\theta)\sin(\phi) + Y/M \\ \dot{w} &= -pv + uq - g\cos(\theta)\cos(\phi) + \left(Z - F_T \sin\alpha_T\right)/M \end{aligned} \tag{12}$$

Where u, v, w are the velocity components on x, y and z body axis; p, q and r are roll, pitch and yaw rate related to body axis; ϕ, θ and ψ are the Euler angles around x, y e z, respectively; α_T is the angle between aircraft longitudinal axis and the engine axis; g is gravity acceleration; M is the aircraft mass and X, Y and Z are the aerodynamic force on each direction, defined as an approximation given by the aerodynamic coefficients. F_T, the propulsive force, is defined through a simple engine model. Replacing variables, Eq. (12) may be written on the aerodynamic referential system as shown on Eq. (13).

ISSN 2176-5480

$$\dot{V} = (u\dot{u} + v\dot{v} + w\dot{w})/V \quad \dot{\alpha} = (u\dot{w} - w\dot{u})/(u^2 + w^2) \quad \dot{\beta} = (V\dot{v} - v\dot{V})/(V\sqrt{V^2 + v^2}) \tag{13}$$

Where V is the resultant velocity, α is the angle of attack and β is sideslip angle. The Moment equations are shown on Eq. (14).

$$\dot{p} = (c_1 r + c_2 p)q + c_3 l + c_4 n \quad \dot{q} = c_5 pr - c_6(p^2 - r^2) + c_7(m - H_T) \quad \dot{r} = (c_8 p - c_2 r)q + c_4 l + c_9 n \tag{14}$$

Where l, m and n are the aerodynamic moments, defined as an approximation given by the aerodynamic coefficients. H_T is the angular moment caused by the engine, also defined through a simple engine model, and c_i coefficients are given by Eq. (15).

$$\begin{aligned} c_1 &= \frac{(I_{yy} - I_{zz})I_{zz} - I_{xz}^2}{I_{xx}I_{zz} - I_{xz}^2} & c_2 &= \frac{(I_{xx} - I_{yy} + I_{zz})I_{xz}}{I_{xx}I_{zz} - I_{xz}^2} & c_3 &= \frac{I_{zz}}{I_{xx}I_{zz} - I_{xz}^2} \\ c_4 &= \frac{I_{xz}}{I_{xx}I_{zz} - I_{xz}^2} & c_5 &= \frac{I_{zz} - I_{xx}}{I_{yy}} & c_6 &= \frac{I_{xz}}{I_{yy}} \\ c_7 &= \frac{1}{I_{yy}} & c_8 &= \frac{(I_{xx} - I_{yy})I_{xx} - I_{xz}^2}{I_{xx}I_{zz} - I_{xz}^2} & c_9 &= \frac{I_{xx}}{I_{xx}I_{zz} - I_{xz}^2} \end{aligned} \tag{15}$$

Where I_{xx}, I_{yy}, I_{zz} and I_{xz} are the inertia moments around each axis. The "Cinematic equations are shown on Eq. (16).

$$\dot{\psi} = (q\sin(\phi) + r\cos(\phi))/\cos(\theta) \quad \dot{\theta} = q\cos(\phi) - r\sin(\phi) \quad \dot{\phi} = p + \tan(\theta)(q\sin(\phi) + r\cos(\phi)) \tag{16}$$

Finally, the navigation equations are shown on Eq. (17).

$$\begin{aligned} \dot{x}_0 &= u\cos(\theta)\cos(\psi) + v(\sin(\phi)\sin(\theta)\cos(\psi) - \cos(\phi)\sin(\psi)) + w(\cos(\phi)\sin(\theta)\cos(\psi) + \sin(\phi)\sin(\psi)) \\ \dot{y}_0 &= u\cos(\theta)\sin(\psi) + v(\sin(\phi)\sin(\theta)\sin(\psi) + \cos(\phi)\cos(\psi)) + w(\cos(\phi)\sin(\theta)\sin(\psi) - \sin(\phi)\cos(\psi)) \\ \dot{H} &= u\sin(\theta) - v\cos(\theta)\sin(\phi) - w\cos(\theta)\cos(\phi) \end{aligned} \tag{17}$$

Where x_0, y_0 and H are the aircraft position related to the inertial reference system. Considering the mass as variable parameter during the flight, one may model its dynamic as shown on Eq. (18)

$$\dot{m} = -c_{mV}F_T \tag{18}$$

Where c_{mV} is the fuel mass specific consumption related to thrust. For the simulations in the present work, one used an atmospheric model based on an approximation of the international standard atmosphere (ISA).

4. AUTOPILOT DESIGN

This section aims to present, implement, simulate and discuss the results of the autopilot projects implemented on the present work.

4.1 Cruise Autopilot

The Cruise Autopilot objective is to keep the aircraft with constant altitude and aerodynamic velocity, while rejecting disturbs. It aims to reduce pilot workload, optimize fuel consumption during cruise and increase the passengers comfort. Its details are shown on the next two subsections.

4.1.1 Altitude Hold Design

The Altitude Hold is an import pilot-relief mode capable to meet air-traffic control requirements. The measured variable is altitude while the control variable is elevator δ_p.

ISSN 2176-5480

For this project, one may use the aircraft longitudinal linearized model, described by the states $[V \quad \gamma \quad \alpha \quad q \quad H]$, where γ, the trajectory angle, may be found replacing variables α and θ on the aircraft complete model. The Stability Augmentation System on the internal loop is based on a feedback of θ and q, a Pitch Hold, since one has the complete longitudinal movement model available. The inner loop control is also done using elevators. A lead compensator is chosen because the open loop plant already has a pole that is close to the origin, able to work as an integrator. The compensator structure and each parameter value are shown on Eq. (19), where the pole in -10 was placed arbitrarily. The control scheme is similar to the one shown in Figure 1; the gains for the SAS are identified by $K_{Y,\theta}$ and $K_{Y,q}$, while the gains for the Altitude Hold are called $K_{V,H,1}$ and $K_{V,H,2}$.

$$\begin{aligned} \dot{w} &= Fw + Ge \\ v &= Dw + Je \end{aligned} \quad F = -10 \quad G = 1 \quad D = \begin{bmatrix} 1 \\ 0 \end{bmatrix} \quad J = \begin{bmatrix} 0 \\ 1 \end{bmatrix} \tag{19}$$

4.1.2 Velocity Hold Design

On the Aerodynamic Velocity Hold, the measured variable is aerodynamic velocity, controlled by the throttle setting π. On the present work this autopilot loop is closed over the Altitude Hold autopilot. So, a SAS is not necessary, once the previous project already have an augmented stability. The velocity is controlled through a Proportional-Integral compensator, since one wishes to track a trajectory of velocity and the open loop system (plant and altitude hold autopilot) is not a type 1 system. The compensator structure and each parameter value are shown on Eq. (20). The gains for the Aerodynamic Velocity Hold are referenced by $K_{V,V,1}$ and $K_{V,V,2}$.

$$\begin{aligned} \dot{w} &= Fw + Ge \\ v &= Dw + Je \end{aligned} \quad F = 0 \quad G = 1 \quad D = \begin{bmatrix} 1 \\ 0 \end{bmatrix} \quad J = \begin{bmatrix} 0 \\ 1 \end{bmatrix} \tag{20}$$

4.1.3 Gains Calculation

The non-linear system model is trimmed in multiple conditions of altitude and mass using the *fsolve* MATLAB® function, able to solve systems of nonlinear equations of several variable. The linear system for each flight condition was then used to find the control law gains. In this case, it was used as method the Linear Quadratic Regulator for Output Tracking with Time-Depending Weighting, described on subsection 2.1.2, since the objective was to eliminate quickly the steady state error of tracking the altitude and velocity trajectory. The weight of the controls usage, R, was regulated as to decrease the thrust (and consequently the fuel consumption) and the actuation over elevators, what could degrade the actuators life cycle. The weight of the time dependent term was increased in order to cancel the steady state error as fast as possible.

The calculated gains are then scheduled for the flight on cruise regime, where one observes the greatest variation of mass. Table 1 shows a partial list of linearization conditions for cruise, the respective list of calculated gains and the gain (GM) and phase margin (PM) for the specific project.

Table 1. Linearization points and calculated gains for Cruise Autopilot

V (m/s)	H (m)	m (kg)	π	$K_{Y,\theta}$	$K_{Y,q}$	$K_{V,H,1}$	$K_{V,H,2}$	$K_{V,V,1}$	$K_{V,V,2}$	GM (dB)	PM (°)
242	9500	120000	0.8	-0.083	-0.912	-0.133	0.014	-0.014	-0.230	Inf	68.1
242	9500	100000	0.8	-0.044	-0.735	-0.140	0.014	-0.014	-0.224	Inf	76.7
250	10000	120000	0.8	-0.040	-0.734	-0.140	0.014	-0.014	-0.261	Inf	76.6
250	10000	100000	0.8	-1.000	-1.000	-1.000	0.108	-0.015	-0.207	Inf	72.6
258	10500	120000	0.8	-1.000	-1.000	-1.000	0.108	-0.016	-0.238	Inf	72.4
258	10500	100000	0.8	-0.995	-0.830	-0.602	0.067	-0.015	-0.213	Inf	72.6

One may observe as conclusion that the gain and phase margins are way above the minimal values, defined by the MIL standards and equivalent to 6 dB and 35 degrees, respectively. This indicates the high robustness of the project.

4.2 Climb and Descent Autopilot

ISSN 2176-5480

The Climb and Descent Autopilot are similar projects. They are both based on an Indicated Airspeed Hold. The differences are, of course, the initial condition and the throttle setting. The Indicated Airspeed (V_{IAS}) formula is shown on Eq. (21). If there is extra throttle, the aircraft will climb, decreasing air density, and, in order to keep its V_{IAS} constant, it will increase its true airspeed. When, on the other hand, there is a lack of throttle, the aircraft will descend and its true airspeed will decrease.

$$V_{IAS} = V\sqrt{\rho/\rho_0} \tag{21}$$

For the Indicated Airspeed Hold, the throttle setting is set constant and the velocity is controlled as to keep the indicated airspeed constant using the elevator δ_p. For the gains calculation, one may use the aircraft longitudinal model linearized in a steady flight condition, described by the states $\begin{bmatrix} V & \alpha & \theta & q & H \end{bmatrix}$ and a proportional-integral controller, shown in Eq. (20), since steady state error must be zero. The Stability Augmentation System on the internal loop is a Pitch Hold controlling the elevator. So the gains for the Indicated Airspeed Hold are $K_{Y,\theta}$, $K_{Y,q}$, $K_{V,V,1}$ and $K_{V,V,2}$.

4.2.1 Gains Calculation

The non-linear system model is trimmed in multiple conditions of altitude and mass using the *fsolve* MATLAB® function. The linear system for each flight condition was then used to find the control law gains. In this case, it was used as method the Linear Quadratic Regulator for Output Tracking without Time-Depending Weighting, described on subsection 2.1.1. This method was able to reduce the steady state error quickly enough, so the simplest method was chosen. The weight of the controls usage, R, was regulated as to decrease the actuation over elevators, what could degrade their life cycle.

The calculated gains are then scheduled for the flight on climb and descent regimes, where the variation of altitude causes a great variation of plant dynamic. Table 2 shows a partial list of linearization conditions for climb, the respective list of calculated gains and the gain (GM) and phase margin (PM) for the specific project. The majority of the descent data was omitted because of space restriction.

Table 2. Linearization points and calculated gains for Climb and Descent Autopilot

V (m/s)	H (m)	m (kg)	π	$K_{Y,\theta}$	$K_{Y,q}$	$K_{V,V,1}$	$K_{V,V,2}$	GM (dB)	PM (°)
Climb Autopilot									
145	0	120000	1.0	-2.000	-0.794	-0.003	-0.178	8.7	52.5
145	0	100000	1.0	-2.000	-1.034	-0.003	-0.188	9.1	50.1
164	2500	120000	1.0	-2.000	-0.715	-0.003	-0.178	8.6	54.3
164	2500	100000	1.0	-2.000	-0.918	-0.003	-0.184	8.8	51.5
187	5000	120000	1.0	-2.000	-0.646	-0.002	-0.180	8.5	56.3
187	5000	100000	1.0	-2.000	-0.810	-0.002	-0.182	8.6	53.5
215	7500	120000	1.0	-2.000	-0.585	-0.002	-0.186	8.5	58.0
215	7500	100000	1.0	-2.000	-0.712	-0.002	-0.184	8.5	56.0
250	10000	120000	1.0	-2.000	-0.526	-0.002	-0.195	8.7	58.5
250	10000	100000	1.0	-2.000	-0.618	-0.002	-0.189	8.5	58.1
Descent Autopilot									
145	0	120000	0.3	-0.221	-0.148	0.000	-0.003	16.2	63.1
145	0	100000	0.3	-0.199	-0.110	0.000	-0.003	16.5	63.0

One may observe as conclusion that the gain and phase margins are above the minimal values, defined by the MIL standards and equivalent to 6 dB and 35 degrees, respectively. This indicates the high robustness of the project.

4.3 Capture Autopilot

The Capture Autopilot creates an altitude and velocity reference as make the transition between climb and cruise and between cruise and descent as smooth as possible. In order to guarantee the tracking of the altitude and velocity

ISSN 2176-5480

trajectory, rejecting eventual disturbances, one may use the Reference Model method, where the aircraft must behavior as an ideal model. In this case, the ideal model is an equation of altitude and velocity of reference, described by Eq. (22).

$$\begin{aligned} \dot{x}_m &= A_m x_m + B_m u_m \\ z_m &= H_m x_m \end{aligned} \tag{22}$$

Where z_m is the desired reference and u_m is a step signal with the desired amplitude. One defines that capture must be shaped as an exponential curve, so $A_m = -1/\tau$, $B_m = 1$ and $H_m = 1$. The time constant τ is defined by the horizontal distance that the aircraft must fly to achieve the final altitude and velocity and by the derivative of the climb and descent where the exponential starts or finishes, respectively. The Autopilot gains will be calculated based on this model, although the trajectory for capture from cruise to descent is an unstable exponential.

4.3.1 Model Following for Altitude

For the model following for altitude tracking, the measured variable is altitude while the control variable is elevator δ_p. The linearized longitudinal model contains the states $\begin{bmatrix} \alpha & \theta & q & H \end{bmatrix}$. The velocity state was removed because it is desirable to control mainly the short period mode, opposite to phugoidal model. The Stability Augmentation System on the internal loop is a Pitch Hold controlling the elevator. A feedforward gain, here referenced by $K_{FF,H}$, is included in order to actuate directly over the reference signal, helping to track the trajectory.

It will be used a lead compensator with an integrator to improve the plant dynamic and track the altitude reference with steady state error zero. Equation (23) was defined based on the architecture in Figure 1 and represents the compensator and each value of its parameters, where the lead compensator pole in -5 was defined arbitrarily. The gains for the SAS are identified by $K_{Y,\theta}$ and $K_{Y,q}$, while the gains for the Altitude Model Following mode are called $K_{V,H,1}$, $K_{V,H,2}$, $K_{V,H,3}$ and the previously named $K_{FF,H}$.

$$\begin{aligned} \dot{w} &= Fw + Ge \\ v &= Dw + Je \end{aligned} \quad F = \begin{bmatrix} -5 & 1 \\ 0 & 0 \end{bmatrix} \quad G = \begin{bmatrix} 0 \\ 1 \end{bmatrix} \quad D = \begin{bmatrix} 1 & 0 \\ 0 & 1 \\ 0 & 0 \end{bmatrix} \quad J = \begin{bmatrix} 0 \\ 0 \\ 1 \end{bmatrix} \quad e = H_{reference} - H = H_m x_m - Hx \tag{23}$$

4.3.2 Model Following for Velocity

For the model following for velocity tracking, the measured variable is aerodynamic velocity, controlled by the throttle setting π. On the present work this autopilot loop is closed over the Model following for Altitude mode. So, a SAS is not necessary, once the previous project already have an augmented stability. The velocity is included back on the states matrix and the system is controlled through a lead compensator with an integrator to improve the dynamic and track the velocity reference with steady state error zero, as in the last case. A feedforward gain, here referenced by $K_{FF,V}$, is included in order to actuate directly over the reference signal, helping to track the trajectory. The compensator structure and each parameter value are shown on Eq. (24). The lead compensator pole in -5 was defined arbitrarily and may be placed optimally in future works. The gains for the Velocity Model Following mode are called $K_{V,V,1}$, $K_{V,V,2}$, $K_{V,V,3}$ and $K_{FF,V}$.

$$\begin{aligned} \dot{w} &= Fw + Ge \\ v &= Dw + Je \end{aligned} \quad F = \begin{bmatrix} -5 & 1 \\ 0 & 0 \end{bmatrix} \quad G = \begin{bmatrix} 0 \\ 1 \end{bmatrix} \quad D = \begin{bmatrix} 1 & 0 \\ 0 & 1 \\ 0 & 0 \end{bmatrix} \quad J = \begin{bmatrix} 0 \\ 0 \\ 1 \end{bmatrix} \quad e = V_{reference} - V = H_m x_m - Hx \tag{24}$$

4.3.3 Gains Calculation

The non-linear system model is trimmed in multiple conditions of altitude and mass using the *fsolve* MATLAB® function. The linear system for each flight condition was then used to find the control law gains. In this case, it was used as method the Linear Quadratic Regulator for Output Tracking with Time-Depending Weighting, described on subsection 2.1.2, since the objective was to eliminate quickly the steady state error of tracking the altitude and velocity trajectory. For the altitude tracking, the criteria for steady state error was smaller, so R, the weight of control usage,

ISSN 2176-5480

was smaller and the weight of time dependent factors was higher. Since great variations of thrust are not recommend because can degrade engine life cycle, the weight of the controls usage for the velocity control was greater.

The calculated gains are then scheduled for the flight on capture regime, where one observes great variation of altitude. Table 3 and Table 4 show a partial list of linearization conditions for capture between climb and cruise and between cruise an descent, the respective list of calculated gains and the gain (GM) and phase margin (PM) for the specific project. The majority of the descent data was omitted because of space restriction.

Table 3. Linearization points and calculated gains for Capture Autopilot for Altitude control

V (m/s)	H (m)	m (kg)	π	$K_{Y,\theta}$	$K_{Y,q}$	$K_{V,H,1}$	$K_{V,H,2}$	$K_{V,H,3}$	$K_{FF,H}$
Capture Climb/Cruise Autopilot									
242	9500	120000	1.0	-0.999	-0.211	0.354	-0.071	0.016	0.000
242	9500	100000	1.0	-0.999	-0.139	0.223	-0.045	0.011	0.000
250	10000	120000	1.0	-0.999	-0.180	0.354	-0.071	0.016	0.000
250	10000	100000	1.0	-0.999	-0.228	0.307	-0.061	0.014	0.000
Capture Cruise/Descent Autopilot									
250	10000	120000	0.8	-0.999	-0.181	0.342	-0.068	0.016	0.000
250	10000	100000	0.8	-0.999	-0.213	0.287	-0.057	0.014	0.000

Table 4. Linearization points and calculated gains for Capture Autopilot for Velocity control

V (m/s)	H (m)	m (kg)	π	$K_{V,V,1}$	$K_{V,V,2}$	$K_{V,V,3}$	$K_{FF,V}$	GM (dB)	PM (°)
Capture Climb/Cruise Autopilot									
242	9500	120000	1.0	-0.163	0.033	-0.101	-0.001	Inf	87.0
242	9500	100000	1.0	-0.172	0.034	-0.100	-0.002	Inf	86.7
250	10000	120000	1.0	-0.160	0.032	-0.100	-0.002	Inf	87.1
250	10000	100000	1.0	-0.168	0.034	-0.100	-0.002	Inf	86.7
Capture Cruise/Descent Autopilot									
250	10000	120000	0.8	-0.156	0.031	-0.103	0.002	Inf	87.2
242	9500	100000	0.8	-0.160	0.032	-0.101	-0.001	Inf	86.7

One may observe as conclusion that the gain and phase margins are way above the minimal values, defined by the MIL standards and equivalent to 6 dB and 35 degrees, respectively. This indicates the high robustness of the project.

4.4 Bank Angle Hold Autopilot

The Bank Angle Hold Autopilot aims to keep a constant bank (or roll) angle, ϕ, under the influence of external disturbances. The bank angle feedback increases stiffness in roll and stabilizes spiral mode, providing an important pilot-relief function for long flights and reducing the risk of a coordinated spiral motion toward the ground.

For this project, one uses a lateral-directional linearized model of the aircraft, whose states are $[\beta \quad \phi \quad p \quad r]$. The bank angle ϕ is used as measured variable and the actuation is done on the ailerons δ_a. A lateral-directional SAS on the inner loop is a Yaw Damper, based on the feedback of roll and yaw rate (p e r) and acting over the ailerons and the rudder, δ_r, respectively. A washout filter, a high pass type, is included on the feedback of yaw rate as to avoid that the feedback tries to eliminate the roll rate that, in cases like the coordinated turn, is different from zero. Therefore, the washout filter avoids that the feedback opposes the pilot command.

The compensator is a Proportional-Integral-Derivative (PID) because the open loop system is not type 1 and the objective is to improve dynamic response. Since PID is an unfeasible transfer function, it was included on the open loop system, as it is possible to see in Eq. (25).

ISSN 2176-5480

$$\begin{aligned} \dot{w} &= Fw + Ge & F &= 0 \\ v &= Dw + Je + Lx + Mu & G &= 1 \end{aligned} \quad D = \begin{bmatrix} 0 \\ 1 \\ 0 \end{bmatrix} \quad J = \begin{bmatrix} 1 \\ 0 \\ 0 \end{bmatrix} \quad L = \begin{bmatrix} 0 \\ 0 \\ -1 \end{bmatrix} HA \quad M = \begin{bmatrix} 0 \\ 0 \\ -1 \end{bmatrix} HB \tag{25}$$

The output of the compensator in Eq. (25) will be, according to Figure 1 architecture, $v = \left[e \quad \int e \quad \dot{e} \right]^T = \left[e \quad w \quad -H\dot{x} \right]^T$. The gains for the SAS are identified by $K_{Y,p}$ and $K_{Y,r}$, while the gains for the Bank Angle Hold autopilot PID compensator are referenced by $K_{V,P}$, $K_{V,I}$ and $K_{V,D}$.

4.4.1 Gains Calculation

The non-linear system model is trimmed in multiple conditions of altitude and mass using the *fsolve* MATLAB® function. The linear system for each flight condition was then used to find the control law gains. It was used as method the ITAE Minimization, described on subsection 2.1.3, because it is as simple as possible and, in this case, meets the requirements, i.e., low steady state error on output tracking, high disturbance rejection and low actuation over ailerons and rudder.

The calculated gains are then scheduled for the whole flight, where the great variations of mass and altitude impacts directly the lateral-directional dynamics, because of its low but existent coupling with longitudinal dynamic. Table 5 shows a partial list of linearization conditions for the flight, the respective list of calculated gains and the gain (GM) and phase margin (PM) for the specific project. The majority of the flight conditions where the aircraft was trimmed are omitted because of space restriction.

Table 5. Linearization points and calculated gains for Bank Angle Hold Autopilot

V (m/s)	H (m)	m (kg)	π	$K_{Y,p}$	$K_{Y,r}$	$K_{V,P}$	$K_{V,I}$	$K_{V,D}$	GM (dB)	PM (°)
145	0	120000	1.0	1.604	-1.999	0.445	0.096	0.577	Inf	61.5
145	0	100000	1.0	1.605	-2.000	0.444	0.092	0.581	Inf	61.5
164	2500	120000	1.0	1.412	-1.999	0.441	0.085	0.584	Inf	61.9
164	2500	100000	1.0	1.413	-1.999	0.440	0.082	0.589	Inf	61.9
187	5000	120000	1.0	1.230	-2.000	0.438	0.075	0.594	Inf	62.2
187	5000	100000	1.0	1.231	-1.999	0.437	0.072	0.598	Inf	62.3

One may observe as conclusion that the gain and phase margins are way above the minimal values, defined by the MIL standards and equivalent to 6 dB and 35 degrees, respectively. This indicates the high robustness of the project.

4.5 Simulation Results

Figure 2 shows a non-linear simulation of all designed autopilot projects integrated to execute a typical flight profile. The aircraft climbs with Climb Autopilot engaged, full throttle and constant indicated airspeed equal to 144.9 m/s up to 9.5 thousand meters, where Capture Autopilot takes control. It will take the aircraft until its cruise altitude, 10 thousand meters, following a profile of altitude and velocity and decreasing its throttle on the way. The Cruise Autopilot holds altitude and keeps the velocity as the same indicated airspeed, 144.9 m/s, while the aircraft flies for a specified time until the capture autopilot is engaged to guarantee the tracking of a reference trajectory of altitude and velocity back to 9,500 meters. The Descent Autopilot is then engaged to land the aircraft with constant indicated airspeed. It is possible to see a maximum tracking error on indicated airspeed of 2%.

ISSN 2176-5480

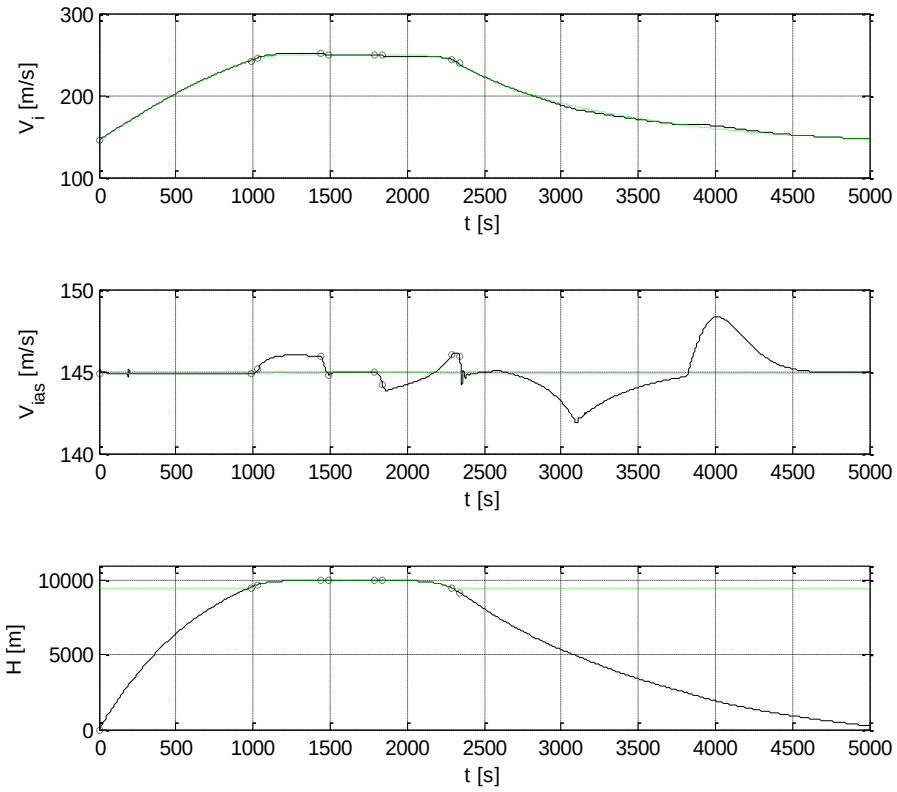

Figure 2. Integrated flight trajectory – Altitude and Velocity

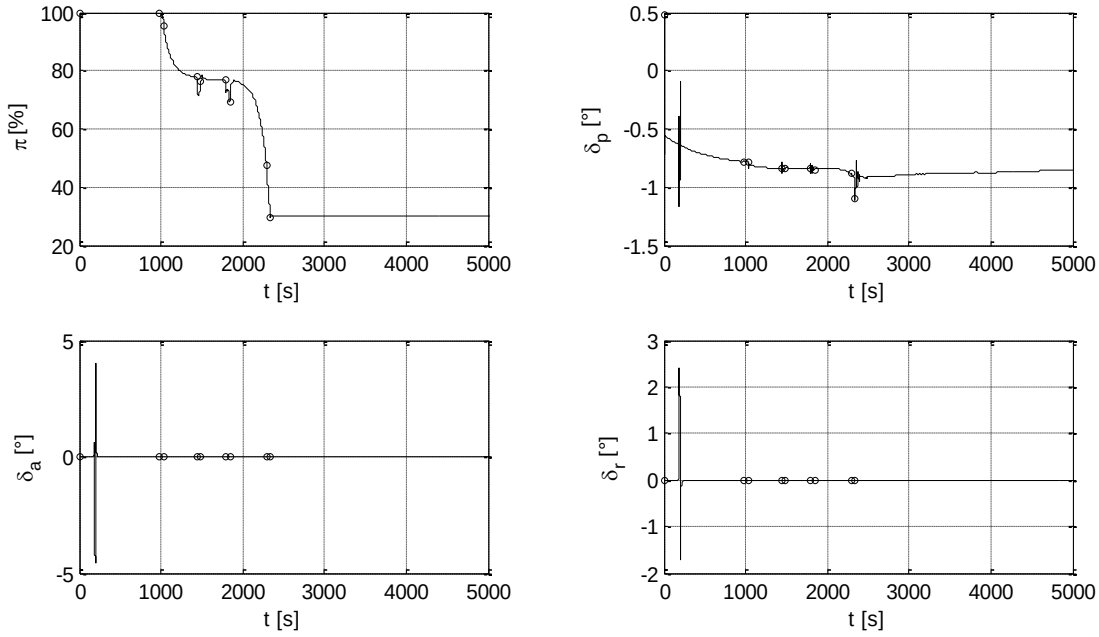

Figure 3. Integrated flight trajectory – Controls

Between each Autopilot engagement, a transition algorithm is used to avoid spikes on the exchange of control between autopilots. An exponential function is used to fade out the current autopilot mode and to fade in the new one. Figure 2 indicates through circles the moment where this exchange of control occurs. Future works may discuss further details regarding the transition algorithm. Figure 3 shows the effect of this algorithm, where it is also possible to see how the controls react in order to reject windshear disturbance applied around 200 seconds. The effect on the lateral-directional movement may be seen in Figure 4.

ISSN 2176-5480

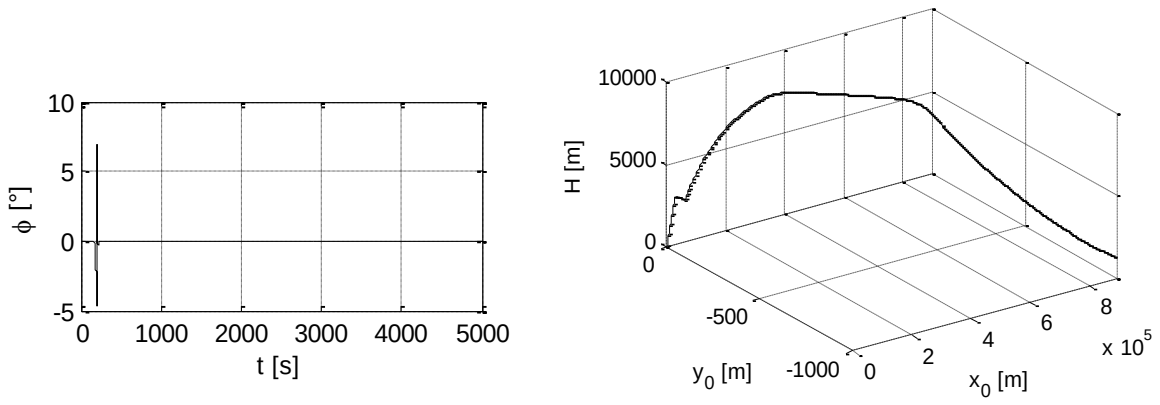

Figure 4. Integrated flight trajectory – Bank Angle and Three Dimensional Movement

Figure 5 shows the variation of mass during the period of the flight and the control law effect on the load factor. It is possible to see that the load factor stays in a safe region for both crew and passengers.

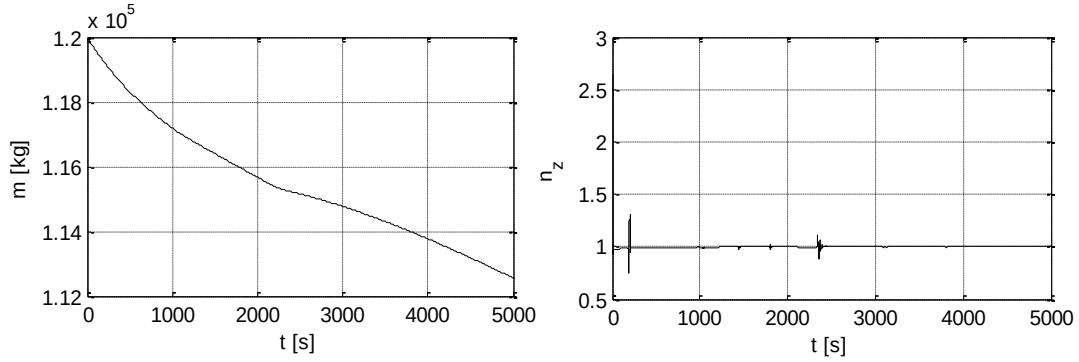

Figure 5. Integrated flight trajectory – load factor (n_z) and mass

5. CONCLUSION

In this paper, the design of a three dimensional autopilot for climb, cruise, descent and capture is presented. The gains are calculated for a series of combinations of altitude and mass, improving the control law ability to cope with the typical changes of dynamics that affects the aircraft during a normal flight. A robustness analysis is done for each trimming condition made throughout the flight envelope validating the project here developed.

Later, a non-linear simulation was able to validate the integrated control laws, to authenticate the effects over the aircraft structure and occupants and to evaluate the controls response as feasible. The integrated project tracked the trajectories as expected and was efficient against a windshear disturbance, meeting this paper main objectives.

6. REFERENCES

Awouda, A. E. A.; Mamat, R. B. *New PID Tuning Rule Using ITAE Criteria*. International Journal of Engineering

Briere, D., Favre, C., & Traverse, P. (2001). *Electrical Flight Controls - From Airbus A320/330/340 to Future Military Transport Aircraft: A Family of Fault-Tolerant Systems*. CRC Press LLC

Etkin, B. (1959). *Dynamics of Flight - Stability and Control*. New York: John Wiley and Sons

Fielding, C. (2000). *The Design of Fly-By-Wire Flight Control Systems*. BAE SYSTEMS (Operations) Limited, Warton Aerodrome, Preston PR4 1AX.

North Atlantic Treaty Organization. (2000). *Flight Control Design - Best Practices*. Québec: Research and Technology Organization

Stevens, B. L., & Lewis, F. L. (1992). *Aircraft Control and Simulation*. Estados Unidos: John Wiley and Sons.

Sutherland, J. P. (1968). *Fly-By-Wire - Flight Control Systems*. Air Force Flight Dynamics Laboratory, Ohio.

7. RESPONSIBILITY NOTICE

The authors are the only responsible for the printed material included in this paper.